JCTC Journal of Chemical Theory and Computation

ARTICLE

pubs.acs.org/JCTC

Assessment of Popular DFT and Semiempirical Molecular Orbital Techniques for Calculating Relative Transition State Energies and Kinetic Product Distributions in Enantioselective Organocatalytic Reactions

Sebastian Schenker,[†,‡] Christopher Schneider,[‡] Svetlana B. Tsogoeva,[‡] and Timothy Clark*[,†,§]

[†]Computer-Chemie-Centrum der Friedrich-Alexander-Universität Erlangen-Nürnberg, Nägelsbachstrasse 25, 91052 Erlangen, Germany

[‡]Lehrstuhl I für Organische Chemie der Friedrich-Alexander-Universität Erlangen-Nürnberg, Henkestrasse 25, 91054 Erlangen, Germany

[§]Centre for Molecular Design, University of Portsmouth, Mercantile House, Portsmouth PO1 2EG, United Kingdom

Supporting Information

ABSTRACT: The performance of computationally accessible levels of calculation for the transition states of organocatalytic reaction has been assessed. Reference post-Hartree−Fock single point energy calculations were used as standards for the gas-phase Born−Oppenheimer relative energies of pairs of alternative transition states that lead to the two product enantiomers. We show that semiempirical methods cannot even be relied on to yield qualitatively correct results. The geometries (optimized, for instance, with DFT) have a large impact on the results of high-level post-HF calculations, so that it is essential to use an adequate DFT technique and basis set. DFT can yield quantitatively correct results that are consistent with post-HF calculations if functionals that consider dispersion are used. Geometries for large systems show larger errors than those for smaller ones but are treated better by functionals such as M06-2X and w97Bxd that include dispersion implicitly or explicitly. Local correlation techniques introduce errors of comparable magnitude to those given by different levels of geometry optimization. We recommend RICC2/TZVP//M06-2X/TZVP, RI-MP2/TZVP// M06-2X/TZVP, and M06-2X/TZVP// M06-2X/TZVP calculations in that order, depending on the size of the system.

INTRODUCTION

Aims. Quantum mechanical calculations have long been important tools in mechanistic organic chemistry. This importance has increased with the availability of accurate modern DFT techniques. Valuable information about the atomistic details of reaction mechanisms that is not available from any other source can be obtained from calculations. Often, the structures and energies of transition states are of most interest. These details of transition states not only tell us qualitatively which reaction pathway is most likely but can also provide a theoretical estimate of the product distribution in the case of kinetic reaction control. Calculations have now advanced to the stage that they can be used to evaluate proposed reaction pathways or to predict the properties of unknown systems, as has been shown successfully for several enantioselective organocatalytic reactions.[1,2] It is therefore of paramount importance to be able to assess the reliability and probable error limits of different calculational methods for typical organic reactions systems. This is especially important as quantum mechanical calculations are now routinely applied to systems large enough that dispersion interactions between nonpolar residues become important.[3−5] Surprisingly, there have been relatively few systematic studies of the quality of commonly used methods. While several methodological benchmarks have been carried out that focus either on achiral activation barriers[6−8] or on relative conformational energies,[9] to our knowledge only two studies on relative enantiomeric or diastereomeric transition-state energies have been carried out to date, by Breslow and co-workers[10] and Simon and Goodman[11] (a concise review of DFT benchmark studies has been published by Ramos et al.[12]). The reaction yield and its enantio- or diastereoselectivity are the quantities of most interest to experimentalists. Whereas the yield is only marginally suitable for theoretical prediction (because it can be affected by many extraneous factors such as competing reactions), selectivities have long been the goal of predictive calculations at many levels.[2,11] We therefore concentrate on this aspect of the calculations, i.e., the difference between activation energies, rather than accurate prediction of their absolute values, because it provides an estimate of the quantity most needed in synthetic research.

Breslow and co-workers concentrated on single-electron transfer and radical reactions, and their primary aim was to optimize predictions of enantioselectivities. Their work considered only two parametrized DFT methods, B3LYP[13] and M06-2X,[14] and concentrated on the suitability of different solvent treatments for improving the quantitative prediction of reaction products. Predictions were good for all systems for which gas-phase UB3LYP/6-31G(d) energies alone gave good agreement with experimental findings, but the authors also noted the shortcomings of their approach for systems in which dispersion interactions are important. In these cases, even the newer of the two functionals, M06-2X,

Received: March 23, 2011
Published: October 03, 2011

Scheme 1. Transition States for the Aldol Reaction Systems 1 and 2

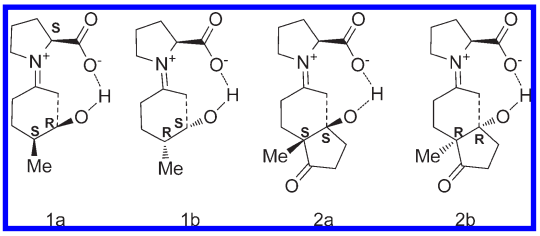

Scheme 2. Transition States for the Aldol Reaction System 3

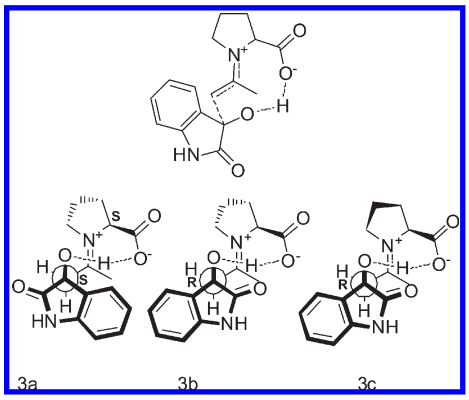

which treats dispersion effects implicitly, did not improve the results. However, the results of this study are unlikely to be applicable to the closed-shell electrophile/nucleophile reactivity usually involved in organocatalysis. As we were carrying out this study, Simon and Goodman reported a benchmark study on a large set of DFT methods, which they used to model known transition states that have been characterized in the literature.[11] They point out that most hybrid and meta-GGA functionals yield similar results for optimized structures. Because they did not carry out high-level reference calculations, they could not identify a recommended functional for optimizations but did focus on the vibrational free-energy corrections for the calculated structures and found that the resolution of the integration grid in the Hessian calculation is vital for accurate free-energy corrections. They also noted that the deviations in energies and geometries can be high throughout the spectrum of functionals.

These two studies,[10,11] while instructive, are limited in that they focus on improving results that already agree well with experimental results. Our aim was to benchmark practical methods with the ultimate aim of predicting stereoselectivity, rather than to find the best corrections to apparently accurate gas-phase Born−Oppenheimer energies. We have therefore focused on a larger set of basis sets, DFT functionals, post-HF methods, and semiempirical Hamiltonians in order to identify practical techniques that agree well with the highest-level calculations. Here, we therefore first consider the fundamental problem of how to calculate good gas-phase data, which can then be combined with appropriate solvent and free-energy corrections to allow us to design versatile computational models for quantitative predictions for a large number of important reactions.

As our aim is to identify reliable computational predictions for routine studies, we focus on four known enantioselective and/or diastereoselective organocatalytic reactions from the work of Houk and Bahmanyar,[15] Tomassini et al.,[16] Papái et al.,[17] and Tsogoeva et al.[18] These are two proline-catalyzed aldol addition reactions with 40−47 atoms in the reaction system, a nitro-Michael reaction *via* an enamine intermediate with 67 atoms, and a thiourea-catalyzed nitro-Michael reaction *via* an amine intermediate with 81 atoms. These varied systems allow us to study the influence of different intermolecular interaction patterns on the quality of the results. While the small proline-catalyzed reactions are dominated by covalent and H-bond interactions, dispersion interactions play a more important role for the larger nitro-Michael reactions.

METHODS

In order to test a wide spectrum of computationally economical techniques, we have investigated three common NDDO-based semiempirical molecular-orbital (MO) techniques, AM1,[19] PM3,[20,21] and PM6;[22] Hartree−Fock (HF) *ab initio* theory; and six popular DFT functionals. The six DFT methods are PBE[23] as a pure generalized gradient approximation (GGA) functional, B3LYP[13] as a hybrid-GGA functional, TPSS[24] and TPSSH[24] as meta-GGA functionals (pure and hybrid), and, as newer representatives, Head-Gordon and Chai's more recent wB97xd functional, which includes an explicit empirical dispersion correction,[25] and M06-2X by Zhao and Truhlar,[14] which implicitly corrects for dispersion and for which very high accuracy for small organic transition states was reported.[26] All DFT calculations were carried out with the Pople 6-31G(d) double-ζ[27,28] and the Ahlrichs TZVP triple-ζ[29] basis sets.

In order to provide benchmark results for comparison, we also performed *ab initio* post-HF single-point calculations. Since direct MP2[30,31] and CCSD[32] scale poorly,[33] we used RI-MP2[34] and RI-CC2[35] (note that RICC2 employs the CC2 approximation[36] in addition to RI). The resolution of identity (RI) approximation allows us to calculate single-point energies even for the largest systems with a polarized triple-ζ basis set. Geometry optimizations beyond RI-MP2 or single-point calculations with larger basis sets on systems of this size remain prohibitive. Unfortunately, CCSD(T), which is often referred to as the "gold standard" in quantum chemistry, is computationally still too costly to be used for the systems considered here.[37] The localized, and therefore theoretically linear scaling, LCCSD(T) ansatz of Werner and Schütz[38−43] was used to test the influence of triple excitations for the electronic energies. LCCSD(T) calculations were performed using Dunning's cc-pVTZ basis set.[44] Different polarized triple-ζ basis sets were used for RI and LCCSD(T) calculations because of the authors' recommended fitting basis sets. We could perform LCCSD(T) single-point calculations for all but the largest system.

CALCULATED TRANSITION STATES IN DETAIL

Aldol Reactions. The transition states used in this study can be divided in two groups, the smaller aldol addition systems and the larger nitro-Michael additions. The first group consists of systems **1** and **2** (Scheme 1) from the work of Houk and Bahmanyar[15] and of system **3** (Scheme 2) from the work of Tomasini et al.[16] Systems **1** and **2** consist, in turn, of two sets of two diastereomeric transition states **1a,b** and **2a,b** (see Scheme 1).

System **3** consists of two diastereomeric transition states **3a,b** and a third **3c**, which only differs from **3b** by a proline ring flip and is known to be very similar in energy to **3b**[16] (see Scheme 2).

Scheme 3. Transition States for the Nitro-Michael System 4

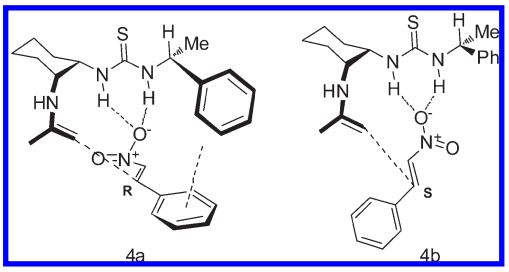

Scheme 4. Transition States for the Nitro-Michael System 5

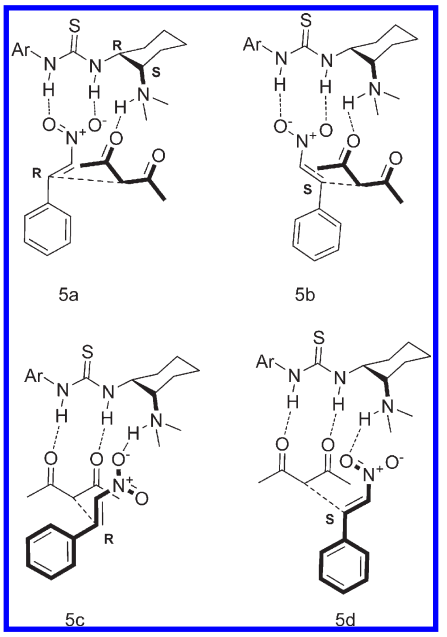

In all cases, the major interactions between the catalyst and the reacting system are either covalent or hydrogen bonds. Both the C−C-bond formation and a simultaneous proton transfer must be described correctly for this reaction. The size of the systems ranges from 41 (20 non-hydrogen) to 67 (33 non-hydrogen) atoms with molecular weights ranging from of 225 g mol^{-1} to 301 g mol^{-1} (i.e., 150−160 electrons; 384−408 basis functions with 6-31G(d) and 526−562 basis functions with TZVP).

Nitro-Michael Reactions. For the larger systems, we used the transition states of two thiourea-catalyzed nitro-Michael reactions, published by Tsogoeva et al. (**4**)[18] and Papai et al. (**5**).[17] The nitro-Michael reaction **4** (Scheme 3) consists of the two diastereomeric transition states **4a** and **4b**. Stereocontrol is achieved mainly by covalent and H-bond interactions. For transition state **4a**, we can also expect the formation of a $\pi-\pi$-interaction pattern between the phenyl groups of the nitrostyrene and the catalyst, in contrast to **4b**, for which this interaction is not possible The size of the system leads us to expect dispersion interactions between the reaction partners to be more important than for the aldol reactions. System **4** consists of 67 atoms (33 non-hydrogen) and has a molecular weight of 464 g mol^{-1} (250 electrons; 643 basis functions with 6-31G(d) and 871 basis functions with TZVP).

For **5** (Scheme 4), two pairs of diastereomeric transition states **5a** and **5b** and **5c** and **5d** were investigated. This system is mainly controlled by H-bond interactions, and we can also expect dispersion interactions to be important. In comparison to **4**, system **5** is expected to show increased flexibility of the alignment of the two reactants at the catalytically active site. This was reported by Pápai et al., who observed low-energy normal modes for bending of the reactants in reactant complexes and the transition state.[17] TS **5** is the largest system considered, with 81 atoms (41 non-hydrogen) and a molecular weight of 662 g mol^{-1} (346 electrons; 831 basis functions with 6-31G(d) and 1123 basis functions with TZVP).

RESULTS AND DISCUSSION

Reference Energies. As definitive a reference calculation as possible is necessary in order to be able to judge the quality of the results. The experimentally observed product distributions can only provide guidance, since the conditions of the gas-phase calculations do not necessarily correspond to the experimental ones. This is particularly important, as small effects (entropy, solvation) can control kinetic enantioselectivity, which reacts extremely sensitively to small changes in activation energies. In our case, gas-phase Born−Oppenheimer geometries and energies are the relevant target properties. We decided to use (RI-) MP2 and CCSD (as RI-CC2 or LCCSD) and local LCCSD(T) single-point calculations as our references. The systematic nature of these post-HF calculations allows us to approach the converged relative energies, so that they provide a good control for the DFT methods. As optimizations with the higher post-HF methods are too expensive, only single-point calculations were used systematically for all systems. However, we were able to optimize systems **1**−**4** using MP2. We expected a large influence of the optimization level on the post-HF energies, so that single-point energies were calculated for the optimized geometries obtained with each functional. The cheaper MP2 single points were carried out on all DFT double-ζ and triple-ζ geometries, while the more extensive RICC2 and LCCSD(T) energy calculations were limited to DFT triple-ζ optimized geometries. All single-point calculations were carried out using augmented triple-ζ basis sets, which are sufficient to give accurate interaction energies and low basis set superposition errors (BSSE).[45] In the ideal case, the CCSD single-point energy differences should not vary strongly for geometries optimized at different levels. Although CCSD/TZVP energies are not definitive, they should not deviate strongly from the "correct" values, so that they provide at least a strong indication of the reliability of other techniques. The same is true for the LCCSD(T)/cc-pVTZ calculations, which are formally more accurate than the CCSD values (because they include a perturbational correction triple excitations) as long as the local-orbital approximation is applicable and accurate enough for our systems.

In order to test whether the local approximation is suitable for our purposes, The MP2 and CCSD single points can be compared with their local LMP2 and LCCSD equivalents. We can safely use the local approximations if the energies agree by significantly less than the change caused by the perturbational triples correction.

All energies discussed in this section are differences between the electronic energies of pairs of transition states optimized at the different DFT levels and are denoted $\Delta\Delta E_{\text{TSA-TSB}}$:

$$\Delta\Delta E_{\text{TSA-TSB}} = \Delta E^*_{\text{A}} - \Delta E^*_{\text{B}} \quad (1)$$

Table 1. Mean Electronic Energy Differences $\Delta\Delta E_{TSA\text{-}TSB}$ with Standard Deviations (all values in kcal mol^{-1})[a]

	DFT	RI-MP2	RI-CC2	L-MP2	LCCSD	LCCSD(T)
1a−1b	*0.81 ± 0.54*	1.49 ± 0.11	1.50 ± 0.15	1.14 ± 0.33	0.54 ± 0.22	0.55 ± 0.25
2a−2b	*3.56 ± 0.86*	5.08 ± 0.25	5.36 ± 0.32	4.93 ± 0.12	4.84 ± 0.35	4.83 ± 0.33
3a−3b	*0.11 ± 0.40*	0.78 ± 0.53	0.68 ± 0.39	0.67 ± 0.83	0.28 ± 1.00	0.72 ± 0.89
3a−3c	*1.02 ± 0.15*	0.97 ± 0.04	1.35 ± 0.17	1.37 ± 0.24	0.79 ± 0.18	0.98 ± 0.11
3b−3c	*1.14 ± 0.37*	1.75 ± 0.54	2.03 ± 0.33	2.04 ± 0.73	1.07 ± 1.11	1.71 ± 0.93
4a−4b	*3.14 ± 1.54*	5.60 ± 1.07	4.87 ± 0.97	3.10 ± 0.77	4.15 ± 0.21	3.58 ± 0.24
5a−5b	*3.79 ± 1.31*	5.46 ± 1.01	6.05 ± 1.24			
5a−5c	*3.27 ± 0.85*	5.39 ± 0.89	5.77 ± 1.34			
5a−5d	*0.17 ± 1.25*	0.97 ± 1.24	1.71 ± 1.36			
5b−5c	*7.06 ± 1.79*	10.85 ± 0.55	11.82 ± 1.14			
5b−5d	*3.96 ± 1.59*	6.42 ± 1.05	7.76 ± 1.15			
5c−5d	*3.09 ± 0.76*	4.43 ± 0.61	4.06 ± 0.66			
			average standard deviation			
all data	0.95	0.66	0.77			
1−4 only	0.64	0.42	0.39	0.50	0.51	0.46

[a] The DFT column shows the statistics for fully optimized geometries using the different DFT methods (PBE, B3LYP, TPSS, TPSSH, w97XD, and M06-2X with the TZVP basis set). The other columns illustrate the effect of using the different DFT-optimized geometries on $\Delta\Delta E_{TSA\text{-}TSB}$ at the given level of theory.

where ΔE_A^* and ΔE_B^* are the calculated Born−Oppenheimer energies for transition states A and B, respectively.

The reason for using this difference as the target value is explained above. We first compare the DFT energy differences with reference values and also the effect of using geometries optimized with different DFT functionals on the corresponding MP2 and CC2 single points. Table 1 shows the mean and the standard deviations of the $\Delta\Delta E$ values from the mean for all pairs of comparable transition states for the DFT/MP2, DFT/CC2, and MP2/CC2 pairs. The mean values indicate how well each calculational level reproduces the values calculated at higher levels, and the standard deviations indicate the spread of the results caused by using different functionals for the DFT methods and the different DFT-optimized geometries for the post-HF calculations.

Table 1 shows that the differences in electronic energy for the pairs of transition states ($\Delta\Delta E$) vary considerably between the methods considered. The variation between the DFT methods is the largest, as expected, because both the geometries and the functionals used vary. For the sets of comparable transition states, the $\Delta\Delta E$ values vary on average by ±0.95 kcal mol^{-1}. For the *ab initio* single points, the deviation is still in the range of ±0.66 (for RI-MP2) to ±0.77 kcal mol^{-1} for (RI-CC2). If the largest system is omitted, the deviation is smaller at ±0.39 (for RI-CC2) to ±0.51 kcal mol^{-1} (for LCCSD). We can thus conclude that the DFT-optimized geometries cause non-negligible differences in the calculated single-point energies for reactivity studies on enantioselective systems. Remarkably, the deviations caused solely by the different geometries in the single-point calculations are almost as high as those found among the DFT methods themselves. Including the largest system, **5**, for which we expect the largest geometric deviations, leads to an increase in the deviation of the single-point energies. The choice of an appropriate economical level of calculation for geometry optimizations is therefore important and will be considered below.

It is known that the errors caused by the RI approximation with accurate fitting basis sets can be kept well below the basis set errors but increase linearly with the number of basis functions.[46] For the systems studied, MP2 optimizations without density fitting were possible for systems **1a**,**b** and **2a**,**b**. An average difference from the RI-MP2 single points of 0.18 kcal mol^{-1} is found, well below the standard deviation of 0.66 kcal mol^{-1} between the RI-MP2 single-point energies (Table 1). We can therefore conclude that the error induced by the RI approximation is well below that introduced by optimizing the geometry at a more economical level of theory.

We also examined whether localized-orbital approximations introduce errors that would affect the accuracy of our predictions for the systems considered. The results are shown in Table 2 with the statistics for the comparison of RI-MP2 and MP2 calculations.

The local-RI and standard-RI results show significant deviations in the energies between LMP2 and MP2 and between LCCSD and RI-CC2. As we can see from Table 2, the deviation for the local approach is always comparable to or significantly larger than the additional perturbational triples corrections. We thus cannot expect to improve the results in our case using the local approach. The most reliable method for single-point energies in this case is thus RI-CC2.

In 11 of the 13 transition states, full optimization at the RI-MP2 level was possible. The root-mean-square difference of interatomic distances (geometric RMS) between all pairs of atoms was used to compare the geometries optimized at the different DFT levels to those optimized with MP2. As shown in Table 3, the best agreement with MP2 geometries is given by M06-2X, with average and maximum geometric RMSDs of only 0.11 Å and 0.27 Å, respectively. The next best functional in terms of the average RMSD is wB97xd (0.31 Å), but it gives the largest RMSD from the MP2 geometry of all (1.47 Å) for transition state **4b**. The same trend can be observed for energies. RI-MP2 single-point energies on DFT-optimized geometries show very good agreement with RI-MP2 optimized energies for M06-2X and wB97xd. RI-MP2 single points on optimizations with M06-2X lie within 2.05 kcal mol^{-1} (maximum error) of the energies obtained for the RI-MP2-optimized geometries (mean error: 0.94 kcal mol^{-1}). For pairs of transition states, the average error cancels out to only 0.16 kcal mol^{-1}. wB97xd performs relatively well. wB97xd/TZVP//RI-MP2/TZVP single-point calculations

Table 2. Mean Absolute Deviation of $\Delta\Delta E$ (kcal mol^{-1}) for Local and Nonlocal Approaches for Pairs of Transition States Compared with the Effect of Higher Order Excitations[a]

	1a−1b	2a−2b	3a−3b	3a−3c	3b−3c	4a−4b	mean ± std dev.
LMP2-MP2	0.40	0.26	0.69	0.36	0.72	1.68	0.69 ± 0.52
LMP2-LCCSD(T)	0.58	0.30	0.46	0.48	0.69	0.73	0.54 ± 0.16
LCCSD-CC2	0.95	0.52	0.75	0.56	1.20	0.74	0.79 ± 0.25
LCCSD-LCCSD(T)	0.13	0.04	0.45	0.19	0.63	0.57	0.34 ± 0.25

[a] As for Table 1, the values given are the mean of the values calculated using all DFT levels for geometry optimization.

Table 3. RMS Difference of Interatomic Distances between Geometries Optimized at the DFT/TZVP and RI-MP2/TZVP Levels (all values in Å) and MP2 Single-Point Energy Differences on Both Geometries, Calculated for Individual Transition States and Pairs of Transition States

RMS difference of interatomic distances [Å]						
	functional					
	PBE	TPSS	B3LYP	TPSSH	M06-2X	wB97xd
average	0.42	0.41	0.47	0.42	0.11	0.31
maximum	1.18	0.93	1.27	1.16	0.27	1.47
energy deviation from the RI-MP2/TZVP: energy differences between pairs of transition states [kcal mol^{-1}]						
	PBE	TPSS	B3LYP	TPSSH	M06-2X	wB97xd
average	0.29	0.48	0.77	0.86	0.16	0.20
maximum	0.90	1.75	2.72	1.72	0.92	0.36
individual TS	5.91	5.40	4.49	3,71	0.94	1.44
average						
maximum	11.26	10.54	9.17	7.52	2.05	2.82

Table 4. Mean Absolute Deviation of $\Delta\Delta E$ Values (kcal mol^{-1}) Calculated with MP2 and CC2 at the DFT-Optimized Geometries from Those Optimized with RI-MP2

	$\Delta\Delta E_{MP2} - \Delta\Delta E_{CC2}$ geometry					
	PBE	TPSS	B3LYP	TPSSH	M06-2X	wB97xd
mean absolute deviation	1.07	1.03	1.18	1.08	0.19	0.19
maximum deviation	3.60	2.97	3.15	2.71	0.54	0.51

show an average deviation in total energy from fully optimized RI-MP2/TZVP calculations of 1.44 kcal mol^{-1}, which cancels out to 0.20 kcal mol^{-1} for the $\Delta\Delta E_{TSA\text{-}TSB}$ energy differences between pairs of transition states.

Table 4 shows that the differences $\Delta\Delta E$ between pairs of transition states for MP2 and CC2 are also smallest for the geometries optimized with M06-2X (mean value: 0.19 kcal mol^{-1}). The same value is found for the geometries optimized with the wB97xd functional. For all other DFT methods, both values increase rapidly. In combination with the excellent agreement of M06-2X geometries with MP2 geometries, these results suggest that geometries optimized with M06-2X are most suitable for higher-level single-point calculations. We have therefore used CC2/TZVP//M06-2X/TZVP energies as the reference for assessing the performance of further methods.

Semiempirical MO Techniques. Semiempirical MO techniques can handle very large systems easily[47] and would therefore be extremely useful for fast scans to provide guidance for experimental studies if the results were reliable enough. Chart 1 shows the results obtained for the semiempirical MO techniques tested.

The results for the different systems vary for the semiempirical methods. While at least qualitatively correct descriptions are possible for the two nitro-Michael reactions, the case for the two aldol reactions is less encouraging. In contrast to a synchronous formation of the new C−C and O−H bonds found in the DFT optimizations, AM1 and PM3 find the reaction proceeds via a multistep path with separated C−C-bond formation and proton-transfer steps, as can be shown by relaxed PES scans along the newly formed C−C and O−H bonds. The energies shown in Chart 1 and listed in Table S1 of the Supporting Information suggest that the qualitative prediction for the selectivity is often, but not reliably and consistently, correct.

Of the semiempirical methods tested, only PM6 gives results that are qualitatively consistent with the DFT calculations for the small systems **1**−**3**. For the larger systems, none of the semiempirical methods give reliable energies. Remarkably, the geometries optimized with PM6 are quite accurate in some cases. The RMSD of all interatomic distances relative to the MP2-optimized geometries is 0.42 Å for **4a** and 0.61 Å for **4b**, comparable to or better than most DFT optimizations for these systems (see Table 6 for DFT results).

DFT-METHODS

Energies. The results shown above suggest that some DFT methods can provide results that are consistent with post-HF ab

Chart 1. $\Delta\Delta E$ (kcal mol^{-1}) Calculated with Semiempirical Molecular Orbital Theory for All Pairs of Transition States[a]

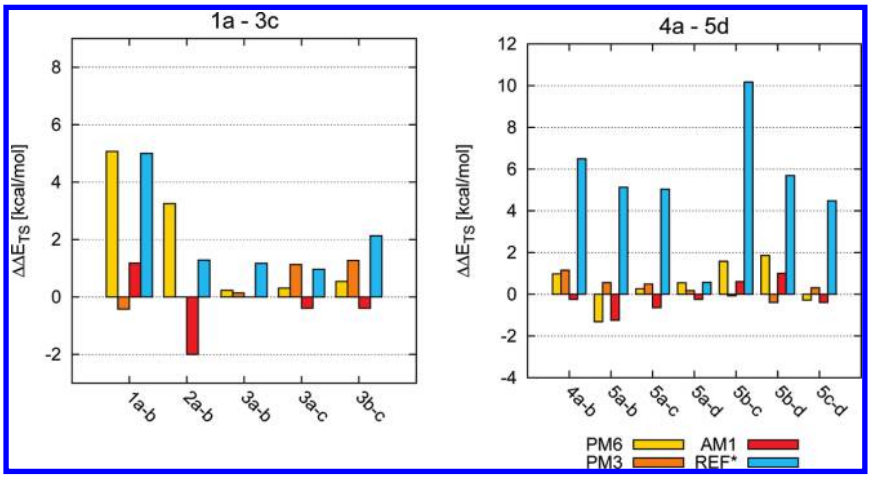

[a]Left: aldol reactions. Right: nitro-Michael reactions. AM1 and PM3 results are estimated from relaxed PES scans because these methods predict multistep reactions. Reference energies calculated at the CC2/TZVP//M06-2X/TZVP level.

Table 5. Mean Absolute Deviation of $\Delta\Delta E$ (kcal mol^{-1}), Calculated at DFT and MP2 Levels Based on DFT Geometries, from the Reference Level (RICC2/TZVP//M06-2X/TZVP) for All Pairs of Transition States

geometry optimization	energy calculation	PBE	TPSS	B3LYP	TPSSH	M06-2X	wB97XD
			all systems				
DFT/6-31G(d)	RI-MP2/TZVP	0.83	1.12	1.01	1.47	0.72	0.44
	DFT/6-31G(d)	1.45	1.38	1.48	1.41	1.28	0.86
DFT/TZVP	RI-MP2/TZVP	0.68	0.67	1.02	0.99	0.20	0.74
	DFT/TZVP	1.88	2.20	2.32	2.15	1.06	0.75
			aldol reactions (1−3)				
DFT/6-31G(d)	RI-MP2/TZVP	0.22	0.67	0.33	1.69	0.06	0.31
	DFT/6-31G(d)	1.02	1.10	1.21	1.14	0.37	0.47
DFT/TZVP	RI-MP2/TZVP	0.19	0.3	0.30	0.99	0.07	0.20
	DFT/TZVP	1.18	1.37	1.63	1.36	0.36	0.53
			nitro-Michael reactions (4−5)				
DFT/6-31G(d)	RI-MP2/TZVP	1.18	1.38	1.39	1.35	1.10	0.50
	DFT/6-31G(d)	1.70	1.54	1.63	1.57	1.80	1.08
DFT/TZVP	RI-MP2/TZVP	0.95	0.88	1.43	0.99	0.26	1.06
	DFT/TZVP	2.28	2.68	2.72	2.60	1.46	0.88

initio data. A question of practical relevance is how to achieve quantitatively correct results at the least computational expense. In this section, we investigate the performance of less computationally expensive methods relative to reference (CC2/TZVP//M06-2X/TZVP) data. We present the results of DFT optimizations with double- and triple-ζ basis sets and MP2/TZVP single points on the DFT-optimized geometries. The calculational protocol can be simplified by calculating MP2 in place of CC2 single points because MP2 is approximately 10 times faster than CC2 for the cases tested. A second possibility is to use the DFT results directly, which avoids the post-HF single point calculations, which are particularly expensive for large systems. If a further increase in efficiency is necessary for the largest systems, either smaller basis sets or less computationally expensive levels of DFT can be used. In particular, pure GGA and meta-GGA calculations can benefit from density fitting in RI approaches, which can lead to an acceleration of up to a factor of ten[48] (>30 in combination with multipole approximations[49]).

Reducing the level of the single-point calculations from CC2 to MP2 hardly affects the results, as shown in Table 5.

Table 5 and Chart 2 (bottom right graph) show that MP2/TZVP//M06-2X/TZVP calculations have an average deviation from the reference energies of only 0.20 kcal mol^{-1} (with only one case with a deviation larger than 0.50 kcal mol^{-1}, data shown in the Supporting Information). Using geometries optimized at other DFT levels leads to a significant degradation in performance, giving both larger average deviations and strong outliers. Only for the small systems (**1**−**3**) is PBE an economical alternative to M06-2X, with an average deviation of 0.19 kcal mol^{-1}

Surprisingly, using a different basis set hardly changes the situation. We expected less accurate energies for single-point calculations on DFT/6-31G(d) optimized geometries. The errors calculated for MP2 single points on DFT-optimized geometries with the TZVP (Chart 2, bottom-right) and 6-31G(d) (Chart 2, top-right) basis sets show that this is true in most

Chart 2. Absolute Deviation and Mean Absolute Deviation (± one standard deviation) of $\Delta\Delta E$ (kcal mol^{-1}) Calculated at DFT and MP2 Levels on the Basis of DFT Geometries, from the Reference System (RICC2/TZVP//M06-2X/TZVP) for All Pairs of Transition States (blue, small systems; yellow, large systems)

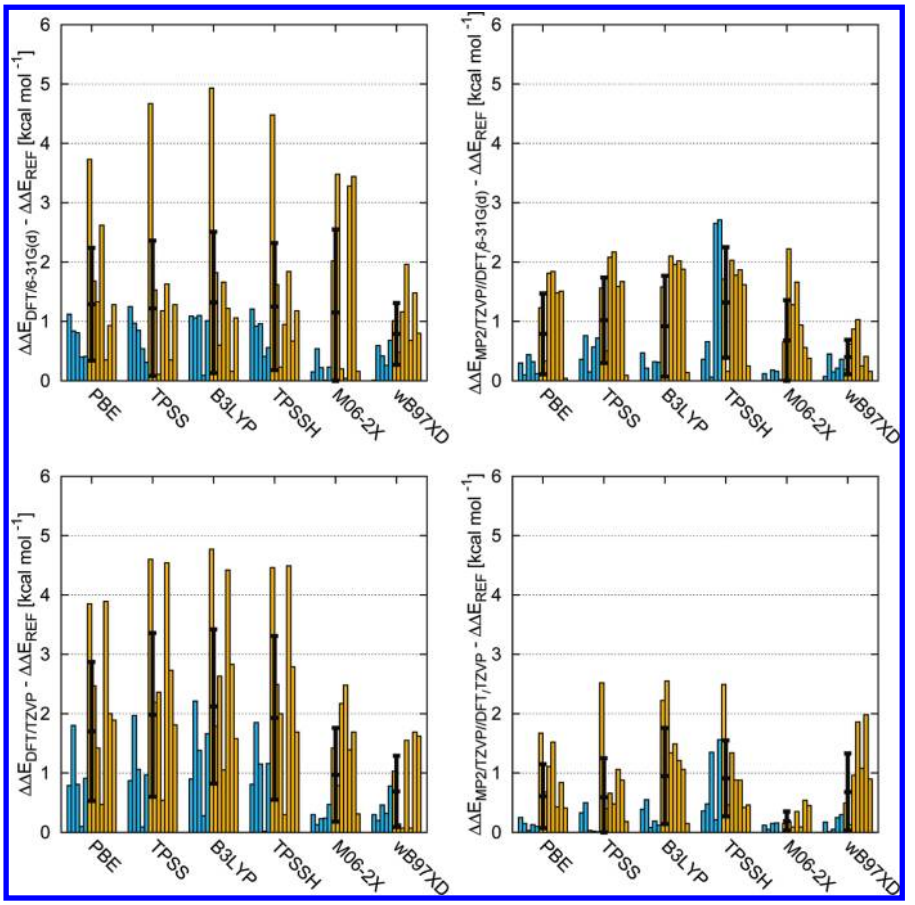

cases. However, the smaller basis set gives lower errors (0.44 kcal mol^{-1}) for wB97xd. These are even better than those found with M06-2X geometries optimized with the smaller basis set (0.72 kcal mol^{-1}).

The computational protocol can be simplified further for vary large systems by using DFT energies. Chart 2 shows that using DFT energies, rather than those from MP2 single points, leads to a significant increase in the deviations from the reference energies. The average deviation is larger than 1 kcal mol^{-1} for all functionals except wB97xd, for which an error of 0.86 kcal mol^{-1} is found with the double-ζ and 0.75 kcal mol^{-1} with the triple-ζ basis set. The M06-2X functional performs marginally less well for energies (mean error = 1.06 kcal mol^{-1} with the TZVP basis set) but might be preferred because it gives better geometries for MP2 single points.

Geometries. For the conventional DFT methods (PBE, B3LYP, TPSS, and TPSSH), energy differences calculated with the double and triple-ζ basis sets do not show any improvement for the triple-ζ basis, but rather the opposite. In order to explain these findings, the similarity of the geometries optimized at the different DFT level was studied. The results are shown in Table 6.

For the small systems **1** and **2**, PBE, TPSS, B3LYP, and TPSSH give consistently better results with the smaller basis set. The opposite is true for M06-2X, and wB97xd performs similarly with the two basis sets. The results are more mixed for the largest aldol reaction **3**, although on balance, optimizations with the larger basis set are slightly better. The larger nitro-Michael reactions **4** and **5** give consistently better results with the larger basis set for all functionals except wB97xd, which performs similarly with the DZ and TZ basis sets. Statistically, M06-2X performs best, followed by wB97xd, as outlined above. However, both, but especially the latter, show a significant degradation in performance as the size of the system increases. Nevertheless, the two functionals that include dispersion implicitly or explicitly perform better for large systems than the others. Dispersion is the probable cause of this effect, although it is possible that MP2/TZVP is overestimating dispersion and therefore contributing to the error.

COMPUTATIONAL METHODS

Semiempirical calculations were carried out using VAMP 10.0.[50] Transition states where characterized by calculating the normal vibrations within the harmonic approximation. Restricted potential energy surface scans for the systems **1**−**3** were carried out using MOPAC09[51] using the distance between the pairs of atoms defining the two newly formed covalent bonds as fixed reaction coordinates in steps of 0.1 Å.

DFT and HF calculations were carried out using Gaussian 09.[52] All transition states were fully optimized using the PBE,[23] TPSS,[24] B3LYP,[13] TPSSH,[24] M06-2X,[14] and wB97xd[25] functionals

Table 6. Comparison of the DFT-Optimized Geometries with MP2/TZVP Optimized Geometries[a]

	RMSD [Å] of all interatomic distances					
functional	PBE	TPSS	B3LYP	TPSSH	M06-2X	wB97xd
basis set	DZ/TZ	DZ/TZ	DZ/TZ	DZ/TZ	DZ/TZ	DZ/TZ
aldol reactions (small systems)						
1a	0.09/0.12	0.09/0.12	0.10/0.14	0.09/0.11	0.10/0.07	0.09/0.10
1b	0.15/0.17	0.17/0.19	0.18/0.2	0.16/0.18	0.06/0.05	0.14/0.14
2a	0.11/0.17	0.14/0.23	0.16/0.24	0.12/0.21	0.07/0.05	0.06/0.05
2b	0.10/0.11	0.09/0.10	0.10/0.11	0.08/0.09	0.04/0.03	0.05/0.04
3a	0.20/0.20	0.21/0.19	0.22/0.19	0.21/0.19	0.15/0.04	0.10/0.09
3b	0.15/0.13	0.17/0.15	0.15/0.18	0.16/0.13	0.05/0.07	0.07/0.07
3c	0.16/0.15	0.18/0.18	0.17/0.15	0.15/0.12	0.08/0.06	0.07/0.06
nitro-Michael reactions (large systems)						
4a	0.76/0.61	0.78/0.62	0.71/0.63	0.77/0.62	0.09/0.14	0.25/0.27
4b	0.64/0.66	0.66/0.68	0.72/0.75	0.65/0.67	0.33/0.22	0.41/0.67
5a	1.25/1.18	1.26/0.93	1.27/0.68	1.27/1.16	0.56/0.27	0.49/0.45
5b	0.99/0.88	1.03/0.89	1.09/0.90	1.09/0.97	1.03/0.23	1.69/1.47
mean	0.42/0.40	0.43/0.39	0.44/0.38	0.43/0.40	0.23/0.11	0.31/0.31
std. dev.	0.42/0.37	0.42/0.32	0.43/0.30	0.44/0.39	0.31/0.09	0.48/0.43

[a] RMSD is calculated as the root-mean square deviation between DFT and MP2 optimized structures for all interatomic distances.

in combination with the 6-31G(d)[27,28] and TZVP[29] basis sets. The transition states were characterized by calculating the normal vibrations within the harmonic approximation. All pure GGA functionals with TZVP basis set were calculated using the density-fitting approach as implemented in Gaussian 09.

RI-MP2 optimizations and RI post-HF single-point calculations were carried out with Turbomole 6.2.[53] All-electron MP2 and CCSD calculations used the RI (resolution of identity) approximated approaches RI-MP2 and RI-CC2 with the (def2-)TZVP[54] basis sets.

All localized correlation methods were carried out with MOLPRO 2010.1[55] using the Dunning cc-pTZV[56] basis set.

The geometrical RMSD between two structures was calculated as the unweighted RMS deviation of all interatomic distances.

CONCLUSIONS

Semiempirical MO theory proved not to be suitable for calculating $\Delta\Delta E$ values, as neither energies nor geometries are accurate enough to describe the reactions correctly.

In comparison, DFT methods perform better. The DFT results are qualitatively correctly rank-ordered for all cases examined, except for those with energy differences lower than 1 kcal mol^{-1}. However, large quantitative differences exist. Only the wB97xd and M062X functionals, which consider dispersion either implicitly or explicitly, gave acceptable energies quantitatively consistent with MP2 and CCSD single points, whereby M06-2X performs best for our test set. CC2/TZVP//M06-2X/TZVP calculations were used as the most reliable reference calculations because M06-2X gives geometries that resemble those obtained with the post-HF ab initio techniques closely.

The gas-phase energy differences for single-point calculations converge to the correct result at the MP2 level of theory; additional explicit correlation hardly improves the results.

BSSE effects can be observed when the smaller (6-31G(d)) basis set is used. Remarkably, using the larger TZVP basis set only improved the results for the modern intrinsic or explicitly dispersion-corrected functionals. For the conventional DFT methods, more accurate energies are found for the smaller basis set. For these functionals, the BSSE contribution apparently cancels part of the missing dispersion energy. Conventional DFT methods give good geometries for small systems, but their performance degrades significantly with increasing system size. This trend is also found with M06-2X and wB97xd but is less pronounced, especially for M06-2X.

We were able to show that geometries optimized with the M06-2X density functional with a triple-ζ basis set can be used in subsequent post-HF single-point calculations to give very accurate gas-phase energies. Our work complements that of Friesner et al.[10] on the best techniques for calculating solvent effects and of Simon and Goodman[11] on accurate free-energy corrections to provide an accurate and economical calculational protocol for predicting the results of kinetically controlled organocatalytic reactions.

We therefore recommend RICC2/TZVP//M06-2X/TZVP, RI-MP2/TZVP//M06-2X/TZVP, and wb97xd/TZVP or M06-2X/TZVP, depending on the size of the system, for calculating energy differences between alternative transition states in stereoselective organocatalytic reactions.

ASSOCIATED CONTENT

Supporting Information. Detailed plot of optimized gas phase energies at the DFT MP2/DFT and CC2/DFT level (Chart S1), Table S1 containing semiempirical transition state energies plotted in Chart 1, gas-phase energies of the individual structures (Table S2−S10) and energy differences between pairs of transition states (Table S11), and geometric RMS and C−C bond length formation data (Table S12). This information is available free of charge via the Internet at http://pubs.acs.org.

AUTHOR INFORMATION

Corresponding Author

*E-mail: Tim.clark@chemie.uni-erlangen.de.

ACKNOWLEDGMENT

We thank the *Deutsche Forschungsgemeinschaft* (SPP 1179) for financial support and the *Leibnitz Rechenzentrum Munich* for computational time and technical support.

REFERENCES

(1) Shinisha, C.; Sunoj, R. Bicyclic proline analogues as organocatalysts for stereoselective aldol reactions: an in silico DFT study. *Org. Biomol. Chem.* **2007**, *5*, 1287–1294.

(2) Houk, K.; Cheong, P. Computational prediction of small-molecule catalysts. *Nature* **2008**, *455*, 309–313.

(3) Grimme, S. Accurate description of van der Waals complexes by density functional theory including empirical corrections. *J. Comput. Chem.* **2004**, *25*, 1463–1473.

(4) Muller-Dethlefs, K.; Hobza, P. Noncovalent interactions: a challenge for experiment and theory. *Chem. Rev.* **2000**, *100*, 143–168.

(5) Morgado, C.; Jure ka, P.; Svozil, D.; Hobza, P.; Šponer, J. Reference MP2/CBS and CCSD(T) quantum-chemical calculations on stacked adenine dimers. Comparison with DFT-D, MP2. 5, SCS

(MI)-MP2, M06-2X, CBS (SCS-D) and force field descriptions. *Phys. Chem. Chem. Phys.* **2010**, *12*, 3522–3534.

(6) Zhao, Y.; Truhlar, D. G. Density Functional Calculations of E2 and SN2 Reactions: Effects of the Choice of Density Functional, Basis Set, and Self-Consistent Iterations. *J. Chem. Theory Comput.* **2010**, *6*, 1104–1108.

(7) Wheeler, S.; Moran, A.; Pieniazek, S.; Houk, K. Accurate Reaction Enthalpies and Sources of Error in DFT Thermochemistry for Aldol, Mannich, and -Aminoxylation Reactions. *J. Chem. Phys. A* **2009**, *113*, 10376–10384.

(8) Zhao, Y.; González-García, N.; Truhlar, D. G. Benchmark Database of Barrier Heights for Heavy Atom Transfer, Nucleophilic Substitution, Association, and Unimolecular Reactions and Its Use to Test Theoretical Methods. *J. Chem. Phys. A* **2005**, *109*, 2012–2018.

(9) Jiang, J.; Wu, Y.; Wang, Z.; Wu, C. Assessing the Performance of Popular Quantum Mechanics and Molecular Mechanics Methods and Revealing the Sequence-Dependent Energetic Features Using 100 Tetrapeptide Models. *J. Chem. Theory Comput.* **2010**, *6*, 1199–1209.

(10) Schneebeli, S. T.; Hall, M. L.; Breslow, R.; Friesner, R. Quantitative DFT Modeling of the Enantiomeric Excess for Dioxirane-Catalyzed Epoxidations. *J. Am. Chem. Soc.* **2009**, *131*, 3965–3973.

(11) Simon, L.; Goodman, J. M. How reliable are DFT transition structures? Comparison of GGA, hybrid-meta-GGA and meta-GGA functionals. *Org. Biomol. Chem.* **2011**, *9*, 689–700.

(12) Sousa, S.; Fernandes, P.; Ramos, M. General performance of density functionals. *J. Chem. Phys. A* **2007**, *111*, 10439–10452.

(13) Becke, A. Density-functional thermochemistry. III. The role of exact exchange. *Chem. Phys.* **1993**, *98*, 5648–5652.

(14) Zhao, Y.; Truhlar, D. The M06 suite of density functionals for main group thermochemistry, thermochemical kinetics, noncovalent interactions, excited states, and transition elements: two new functionals and systematic testing of four M06-class functionals and 12 other functionals. *Theor. Chem. Acc.* **2008**, *120*, 215–241.

(15) Bahmanyar, S.; Houk, K. The origin of stereoselectivity in proline-catalyzed intramolecular aldol reactions. *J. Am. Chem. Soc.* **2001**, *123*, 12911–12912.

(16) Corrêa, R.; Garden, S.; Angelici, G.; Tomasini, C. A DFT and AIM Study of the Proline-Catalyzed Asymmetric Cross-Aldol Addition of Acetone to Isatins: A Rationalization for the Reversal of Chirality. *Eur. J. Org. Chem.* **2008**, *2008*, 736–744.

(17) Hamza, A.; Schubert, G.; Soós, T.; Pápai, I. Theoretical Studies on the Bifunctionality of Chiral Thiourea-Based Organocatalysts: Competing Routes to C- C Bond Formation. *J. Am. Chem. Soc.* **2006**, *128*, 13151–13160.

(18) Yalalov, D.; Tsogoeva, S.; Schmatz, S. Chiral thiourea-based bifunctional organocatalysts in the asymmetric Nitro-Michael addition: a joint experimental-theoretical study. *Adv. Syth. Catal.* **2006**, *348*, 826–832.

(19) Dewar, M.; Zoebisch, E.; Healy, E.; Stewart, J. Development and use of quantum mechanical molecular models. 76. AM1: a new general purpose quantum mechanical molecular model. *J. Am. Chem. Soc.* **1985**, *107*, 3902–3909.

(20) Stewart, J. Optimization of parameters for semiempirical methods I. Method. *J. Comput. Chem.* **1989**, *10*, 209–220.

(21) Stewart, J. Optimization of parameters for semiempirical methods II. Applications. *J. Comput. Chem.* **1989**, *10*, 221–264.

(22) Stewart, J. Optimization of parameters for semiempirical methods V: modification of NDDO approximations and application to 70 elements. *J. Mol. Model.* **2007**, *13*, 1173–1213.

(23) Perdew, J.; Burke, K.; Ernzerhof, M. Generalized gradient approximation made simple. *Phys. Rev. Lett.* **1996**, *77*, 3865–3868.

(24) Tao, J.; Perdew, J.; Staroverov, V.; Scuseria, G. Climbing the density functional ladder: Nonempirical meta−generalized gradient approximation designed for molecules and solids. *Phys. Rev. Lett.* **2003**, *91*, 146401.

(25) Chai, J.; Head-Gordon, M. Long-range corrected hybrid density functionals with damped atom-atom dispersion corrections. *Phys. Chem. Chem. Phys.* **2008**, *10*, 6615–6620.

(26) Xu, X.; Alecu, I. M.; Truhlar, D. G. How Well Can Modern Density Functionals Predict Internuclear Distances at Transition States? *J. Chem. Theory Comput.* **2011**, *7*, 1667–1676.

(27) Rassolov, V.; Ratner, M.; Pople, J.; Redfern, P.; Curtiss, L. 6 31G* basis set for third row atoms. *J. Comput. Chem.* **2001**, *22*, 976–984.

(28) Rassolov, V.; Pople, J.; Ratner, M.; Windus, T. 6-31G basis set for atoms K through Zn. *J. Chem. Phys.* **1998**, *109*, 1223–1229.

(29) Schäfer, A.; Huber, C.; Ahlrichs, R. Fully optimized contracted Gaussian basis sets of triple zeta valence quality for atoms Li to Kr. *J. Chem. Phys.* **1994**, *100*, 5829–5835.

(30) Møller, C.; Plesset, M. Note on an approximation treatment for many-electron systems. *Phys. Rev.* **1934**, *46*, 618–622.

(31) Head-Gordon, M.; Pople, J.; Frisch, M. MP2 energy evaluation by direct methods. *Chem. Phys. Lett.* **1988**, *153*, 503–506.

(32) Cizek, J.; Paldus, J. Coupled Cluster Approach. *Phys. Scr.* **1980**, *21*, 251–254.

(33) Cramer, C. *Essentials of computational chemistry: theories and models*; John Wiley & Sons Inc: New York, 2004; pp 203−248.

(34) Weigend, F.; Häser, M. RI-MP2: first derivatives and global consistency. *Theor. Chem. Acc.* **1997**, *97*, 331–340.

(35) Hättig, C.; Weigend, F. CC2 excitation energy calculations on large molecules using the resolution of the identity approximation. *J. Chem. Phys.* **2000**, *113*, 5154–5161.

(36) Christiansen, O.; Koch, H.; Jørgensen, P. The second-order approximate coupled cluster singles and doubles model CC2. *Chem. Phys. Lett.* **1995**, *243*, 409–418.

(37) Head-Gordon, M. In 10th American Conference on Theoretical Chemistry, Boulder, CO, 1999.

(38) Schütz, M. Low-order scaling local electron correlation methods. V. Connected triples beyond (T): Linear scaling local CCSDT-1b. *J. Chem. Phys.* **2002**, *116*, 8772–8785.

(39) Schütz, M.; Werner, H. Local perturbative triples correction (T) with linear cost scaling. *Chem. Phys. Lett.* **2000**, *318*, 370–378.

(40) Schütz, M.; Werner, H. Low-order scaling local electron correlation methods. IV. Linear scaling local coupled-cluster (LCCSD). *J. Chem. Phys.* **2001**, *114*, 661–681.

(41) Schütz, M. A new, fast, semi-direct implementation of linear scaling local coupled cluster theory. *Phys. Chem. Chem. Phys.* **2002**, *4*, 3941–3947.

(42) Schütz, M. Low-order scaling local electron correlation methods. III. Linear scaling local perturbative triples correction (T). *J. Chem. Phys.* **2000**, *113*, 9986–10001.

(43) Hampel, C.; Werner, H. Local treatment of electron correlation in coupled cluster theory. *J. Chem. Phys.* **1996**, *104*, 6286–6297.

(44) Kendall, R.; Dunning, T., Jr.; Harrison, R. Electron affinities of the first row atoms revisited. Systematic basis sets and wave functions. *J. Chem. Phys.* **1992**, *96*, 6796–6806.

(45) Jurečka, P.; Černý, J.; Hobza, P.; Salahub, D. R. Density functional theory augmented with an empirical dispersion term. Interaction energies and geometries of 80 noncovalent complexes compared with ab initio quantum mechanics calculations. *J. Comput. Chem.* **2007**, *28*, 555–569.

(46) Skylaris, C. K.; Gagliardi, L.; Handy, N. C.; Ioannou, A. G.; Spencer, S.; Willetts, A. On the resolution of identity Coulomb energy approximation in density functional theory. *THEOCHEM* **2000**, *501−502*, 229–239.

(47) Clark, T.; Stewart, J. J. P., MNDO-like Semiempirical Molecular Orbital Theory and its Application to Large Systems. In *Computational Methods for Large Systems*; Reimers, J. J., Ed.; Wiley: Chichester, U. K., 2011; pp 259−286.

(48) Sundholm, D. Density functional theory calculations of the visible spectrum of chlorophyll a. *Chem. Phys. Lett.* **1999**, *302*, 480–484.

(49) Sierka, M.; Hogekamp, A.; Ahlrichs, R. Fast evaluation of the Coulomb potential for electron densities using multipole accelerated resolution of identity approximation. *J. Chem. Phys.* **2003**, *118*, 9136–9148.

(50) Clark, T.; Alex, A.; Beck, B.; Burckhardt, F.; Chandrasekhar, J.; Gedeck, P.; Horn, A.; Hutter, M.; Martin, B.; Rauhut, G.; Sauer, W.;

Schindler, T.; Steinke, T. *VAMP*, 10.0; Accelrys Inc.: San Diego, CA, 2007.

(51) Stewart, J. J. P. *MOPAC2009*; Stewart Computational Chemistry: Colorado Springs, CO, 2008.

(52) Frisch, M. J.; Schlegel, H. B.; Scuseria, G. E.; Robb, M. A.; Cheeseman, J. R.; Scalmani, G.; Barone, V.; Mennucci, B.; Petersson, G. A.; Nakatsuji, H.; Caricato, M.; Li, X.; Hratchian, H. P.; Izmaylov, A. F.; Bloino, J.; Zheng, G.; Sonnenberg, J. L.; Hada, M.; Ehara, M.; Toyota, K.; Fukuda, R.; Hasegawa, J.; Ishida, M.; Nakajima, T.; Honda, Y.; Kitao, O.; Nakai, H.; Vreven, T.; Montgomery, J. A., Jr.; Peralta, J. E.; Ogliaro, F.; Bearpark, M.; Heyd, J. J.; Brothers, E.; Kudin, K. N.; Staroverov, V. N.; Kobayashi, R.; Normand, J.; Raghavachari, K.; Rendell, A.; Burant, J. C.; Iyengar, S. S.; Tomasi, J.; Cossi, M.; Rega, N.; Millam, J. M.; Klene, M.; Knox, J. E.; Cross, J. B.; Bakken, V.; Adamo, C.; Jaramillo, J.; Gomperts, R.; Stratmann, R. E.; Yazyev, O.; Austin, A. J.; Cammi, R.; Pomelli, C.; Ochterski, J. W.; Martin, R. L.; Morokuma, K.; Zakrzewski, V. G.; Voth, G. A.; Salvador, P.; Dannenberg, J. J.; Dapprich, S.; Daniels, A. D.; Ö. Farkas, Foresman, J. B.; Ortiz, J. V.; Cioslowski, J.; Fox, D. J. *Gaussian 09*, Revision A.02; Gaussian, Inc.: Wallingford, CT, 2009.

(53) *TURBOMOLE*, V6.2; TURBOMOLE GmbH: Karlsruhe, Germany, 2010.

(54) Weigend, F.; Ahlrichs, R. Balanced basis sets of split valence, triple zeta valence and quadruple zeta valence quality for H to Rn: Design and assessment of accuracy. *Phys. Chem. Chem. Phys.* **2005**, *7*, 3297–3305.

(55) Werner, H.-J.; Knowles, P. J.; Manby, F. R.; Schütz, M.; Celani, P.; Knizia, G.; Korona, T.; Lindh, R.; Mitrushenkov, A.; Rauhut, G.; Adler, T. B.; Amos, R. D.; Bernhardsson, A.; Berning, A.; Cooper, D. L.; Deegan, M. J. O.; Dobbyn, A. J.; Eckert, F.; Goll, E.; Hampel, C.; Hesselmann, A.; Hetzer, G.; Hrenar, T.; Jansen, G.; Köppl, C.; Liu, Y.; Lloyd, A. W.; Mata, R. A.; May, A. J.; McNicholas, S. J.; Meyer, W.; Mura, M. E.; Nicklass, A.; Palmieri, P.; Pflüger, K.; Pitzer, R.; Reiher, M.; Shiozaki, T.; Stoll, H.; Stone, A. J.; Tarroni, R.; Thorsteinsson, T.; Wang, M.; Wolf, A. *MOLPRO*, 2010.1; Cardiff University: Cardiff, Wales, 2010.

(56) Dunning, T. H. Correlation Consistent Basis Sets. *J. Chem. Phys.* **1989**, *90*, 1007–1023.